Catal Lett (2012) 142:875–881
DOI 10.1007/s10562-012-0827-z

Mixed MgAl Oxide Supported Potassium Promoted Molybdenum Sulfide as a Selective Catalyst for Higher Alcohol Synthesis from Syngas

MoS_2/K_2CO_3 on Mixed Metal Oxides for Higher Alcohol Synthesis

Michael R. Morrill · Nguyen Tien Thao · Pradeep K. Agrawal · Christopher W. Jones · Robert J. Davis · Heng Shou · David G. Barton · Daniela Ferrari

Received: 17 January 2012 / Accepted: 13 April 2012 / Published online: 26 May 2012

Abstract A Mg/Al mixed metal oxide material (MMO) is introduced as a support for K_2CO_3 promoted MoS_2 in CO hydrogenation reactions at 310 °C and 1,500 psig. The catalyst is shown to be more selective for C_2–C_4 linear alcohols (substantially so for C_3–C_4 linear alcohols) than for methanol and offers good alcohol to hydrocarbon selectivity. Methanol selectivity of the MMO supported catalyst deviates greatly from the Anderson–Shultz–Flory distribution.

Keywords Syngas · Higher Alcohols · Molybdenum Sulfide · Mixed Metal Oxide · Hydrotalcite

1 Introduction

Syngas has been converted into long chain hydrocarbons [1, 2] and methanol [3, 4] on a commercial scale for a number of years. In recent years, there has been renewed interest in the conversion of syngas into higher alcohols. Higher terminal alcohols including ethanol, 1-propanol and 1-butanol are increasingly used as fuel additives and chemicals.

A variety of catalysts have been evaluated for the conversion of syngas to higher alcohols [5]. These catalysts include modified Fischer–Tropsch or methanol synthesis catalysts, which are typically adapted for alcohol synthesis by adding promoters such as alkali or other transition metals. Another class of catalysts developed in the late 1980s for these reactions is based on alkali promoted molybdenum sulfide [6–9] which is commonly combined with cobalt [10–13]. While molybdenum sulfide based catalysts facilitate reactions that are largely selective for alcohols, their catalytic activity relative to noble metal catalysts, such as those based on Rh, is lower [14–19]. This is offset by the comparatively lower cost of molybdenum based systems relative to many other metal-based systems. Molybdenum sulfide based catalysts also typically require comparatively high reaction pressures, often up to 2,000 psig, to achieve useful catalytic productivities.

Michael R. Morrill and Nguyen Tien Thao contributed equally to this work.

Electronic supplementary material The online version of this article (doi:10.1007/s10562-012-0827-z) contains supplementary material, which is available to authorized users.

M. R. Morrill · N. T. Thao · P. K. Agrawal (✉) · C. W. Jones (✉)
School of Chemical & Biomolecular Engineering, Georgia Institute of Technology, 311 Ferst Dr. NW, Atlanta, GA 30332, USA
e-mail: Pradeep.agrawal@chbe.gatech.edu

C. W. Jones
e-mail: cjones@chbe.gatech.edu

Present Address:
N. T. Thao
Faculty of Chemistry, Vietnam National University, 19-Le Thanh Tong ST, Hanoi, Vietnam

R. J. Davis · H. Shou
Chemical Engineering Department, University of Virginia, Charlottesville, VA 22904, USA

D. G. Barton
Core R&D, The Dow Chemical Company, Midland, MI 48674, USA

D. Ferrari
Hydrocarbons R&D B-251/7, The Dow Chemical Company, 2301 N Brazosport Blvd., Freeport, TX 77451, USA

Potassium-promoted molybdenum sulfide remains an important benchmark catalyst for higher alcohol synthesis. In attempts to improve these catalysts, many reports describe alkali-promoted molybdenum sulfide phases on high surface area supports, including alumina, silica, carbon nanotubes, activated carbon, and clay [3, 20–29]. In some cases higher alcohol productivity per gram of Mo was slightly improved while in others, higher alcohol selectivity was improved.

Acidic supports such as γ-alumina have been previously shown to yield more hydrocarbons than more neutral or basic supports such as activated carbon, silica, or magnesia [30, 31]. It is believed that the acid sites promote coking, isomerization, and alcohol dehydration [24, 32]. Consequently, basic promoters can be added to a catalyst to neutralize acidic sites and promote C–C and C–O bond formation [16]. Potassium is the most effective promoter for higher alcohol synthesis, most often applied in the form of potassium carbonate [33, 34], and is suggested to promote alcohol formation by limiting CO dissociation or by controlling hydrogenation rates, both of which affect the population of intermediates formed on the catalyst surface [6, 8, 33, 35, 36]. However, alkali promotion is also known to lower catalyst activity—an effect attributed to the blockage of active sites [28, 33, 37].

We hypothesized that the combination of potassium as a promoter with intrinsically basic, high surface area supports may lead to new supported catalysts with improved alcohol selectivity. To this end, two basic supports, a lab-synthesized MgAl mixed metal oxide (MMO) [38–40] derived from a hydrotalcite precursor and a commercial magnesium silicate sepiolite were applied as supports for potassium-promoted molybdenum sulfide. As benchmarks, potassium-promoted bulk molybdenum sulfide and potassium-promoted molybdenum sulfide supported on activated carbon were also evaluated. Of these catalysts, the MMO supported catalyst is shown to be a promising new composition for producing higher alcohols, with the product distribution biased sharply towards production of C^{2+} alcohols at the expense of methanol.

2 Experimental

Activated carbon and sepiolite were obtained from commercial sources (Aldrich and Tulsa respectively). The MMO support was synthesized using methods similar to those described in the literature [41–43]. In brief, three solutions were prepared—A, B, and C. Magnesium nitrate hexahydrate (Alfa Aesar, 98–102 %), aluminum nitrate nonahydrate (Alfa Aesar, 98–102 %), and distilled water were combined with an approximate Mg:Al molar ratio of 7:3 and 0.6 M in metal ions to make solution A. Solutions B and C were 1.2 M NaOH (EMD, 97.0 %) and 0.15 M Na_2CO_3 (Aldrich, 99.5+ %) respectively.

First, 100 mL of solution C was heated to 65 °C and stirred. 360 mL of solutions A and B were then added simultaneously to C at a constant flow rate of approximately 11 mL/min with constant stirring. The flow rate of solution B was varied to maintain a mixture pH of 9.5+/− 0.05 measured with an Oakton 110 series pH meter. After the addition of solutions A and B, the resultant mixture was stirred for 24 h at 65 °C, filtered at room temperature, washed with 2 L of distilled water, and dried overnight at 105 °C. To convert the material from hydrotalcite to MMO, it was ground with a mortar and pestle and heated in air to 450 °C at 5 °C/min and held for 2 h.

Supported MoO_3 was synthesized on the various carriers by an identical incipient wetness impregnation procedure followed by a thermal treatment. To prevent hydrotalcite "memory" effects [44, 45] which potentially reduce catalytic activity by increasing crystallite size and "burying" promoters [14–16, 45], DMSO (Aldrich, 99.9+ %) was used as the impregnation solvent. Targeting approximately 7 wt%. Mo, an appropriate amount of ammonium molybdate tetrahydrate (AMT) (Aldrich, ACS Reagent) and DMSO were combined and stirred at room temperature until the AMT was dissolved. The solution was then added to the support and heated at 135 °C for 12 h in open atmosphere. The resultant solid was then placed in a quartz tube and heated to 450 °C for 2 h with a heating rate of 5 °C/min under 40 mL/min of flowing nitrogen. The sample was then cooled to room temperature and stored in a sealed vial and filled with argon. These samples consisted primarily of MoO_3 dispersed on the support.

Bulk molybdenum sulfide was prepared from methods described in the literature [46]. AMT and 20 % $(NH_4)_2S$ (Alfa Aesar, 20–24 % aq.) were combined and stirred for 1 h at 65 °C. A 25 wt% acetic acid solution was then added to the mixture to precipitate the thiomolybdate. After allowing the mixture to cool, it was filtered and washed with distilled water. The compound was then decomposed by heating at 5 °C/min to 450 °C under 40 mL/min flowing nitrogen for 2 h to form MoS_2.

Before use in catalytic reactions, K_2CO_3 (Sigma-Aldrich, 99 %), previously treated at 105 °C, was added to the supported MoO_3 or unsupported MoS_2 and ground using a mortar and pestle for 15 min. The mixture was pressed into 10 mm pellets at 1,000 psig, crushed, and sieved to 20–40 mesh. The catalyst was then loaded into a ¼″ steel tube with a layer of SiC (Alfa-Aesar, 46 grit) at its base and flushed with nitrogen in a downflow configuration.

Before reaction with syngas, 10 % H_2S/H_2 (Matheson Tri-Gas, UHP) was passed over the catalyst at 40 mL/min. Under this flow, the bed was heated from 22 °C and 15 psig to 450 °C at 5 °C/min and held for 2 h. While still

under 40 mL/min H_2S/H_2 flow, the bed was allowed to cool to 310 °C. Finally, the reactor was flushed with syngas, 1:1 H_2 (Airgas, UHP):CO (Airgas, UHP, 10 % N_2 as an internal standard), and 50 ppm H_2S (diluted down from 3,000 ppm H_2S in He, Matheson Tri-Gas, UHP), purified with a zeolite 5 A molecular sieve carbonyl trap) at 100 mL/min for 5 min and then pressurized to 1,500 psig. Reactions were carried out until activity and product selectivity stabilized, which typically took 2–4 days. An Agilent 7,890 gas chromatograph was used to quantify reaction products. Specifically, methane, ethane, propane, butane, ethylene, carbon dioxide, methanol, ethanol, *n*-propanol, iso-propanol, *n*-butanol, iso-butanol, methyl acetate, ethyl acetate, methyl formate, and ethyl formate were quantified using single point calibration curves. CO conversion, product yields and selectivities were calculated from pseudo-steady-state data. The space velocity was adjusted by varying the syngas flow rate until a conversion of ca. 8 % was reached. An H_2S concentration of 50 ppm was maintained in the syngas feed [34, 47].[1]

The catalysts, precatalysts and supports were characterized via nitrogen physisorption, powder X-ray diffraction, Raman spectroscopy, and temperature programmed desorption (TPD) of CO_2 and NH_3. All post-reaction catalysts were characterized ex-situ after in-situ passivation via 1 % O_2 in He (Matheson Tri-Gas, UHP) for 6 h at room temperature while flowing at 40 mL/min. Elemental analysis was performed with a Perkin Elmer Optima 7300 DV equipped with an optical emission spectrometer. Aliquots of each catalyst were digested in an H_2O_2/HNO_3 solution and then analyzed in duplicate.

Surface areas were calculated from nitrogen physisorption data obtained at 77 K using a Micromeritics Tristar II. All samples were heated to 200 °C under vacuum for 10 h before analysis. Powdered X-ray diffraction was performed using a Philips X-pert diffractometer using CuKα radiation.

Basic sites were quantified via temperature-programmed desorption of CO_2 using a Micromeritics Autochem II. In these experiments, ca. 0.12 g of sample was loaded into a quartz sample tube. Helium (Airgas, UHP) was passed over the sample at 50 mL/min to pretreat each material as it was heated to 700 °C at 10 °C/min. The sample was then cooled to 50 °C and exposed to pure CO_2 (Airgas, research grade) at 50 mL/min for 2 h. The tube was then flushed again with He at 50 °C/min for 1 h. Finally the sample was heated (under flowing He) to 700 °C at 10 °C/min, and a TCD was used to quantify the desorbing gas. Acid sites were quantified using the same instrument, but using 2 % NH_3 in N_2 (Matheson-Trigas, 1.871 % NH_3) as the probe molecule. The TPD procedure was identical to that of the CO_2 TPD, except that sample was heated only to 450 °C, cooled to 100 °C, then exposed to 2 % NH_3/N_2, and heated again to 450 °C.

Raman spectra were obtained using a Witec confocal Raman microscope (Alpha 300R) with an Ar^+ ion laser ($\lambda = 514.5$ nm) with 1 mW of intensity from the excitation source.

3 Results and Discussion

XRD patterns of the synthesized materials are shown in Fig. 1. The bulk MoS_2 pattern showed distinct 002, 100, 103, 105, and 110 MoS_2 planes. Peaks associated with the 100 and 110 planes could also be observed in the activated carbon and MMO supported samples, though they were substantially less intense, indicating smaller and/or less crystalline domains. Features associated with MoS_2 planes were not discernible on the sepiolite supported sample, possibly because they overlapped with the pattern of the support itself.

Raman spectroscopy also revealed the presence of MoS_2 domains as shown in Fig. 2. In all but the activated carbon supported sample, characteristic [48] Mo–S stretching bands were readily observable at 380 and 408 cm^{-1}. The estimated resolution of the spectrometer is $\sim$2 cm^{-1}, and

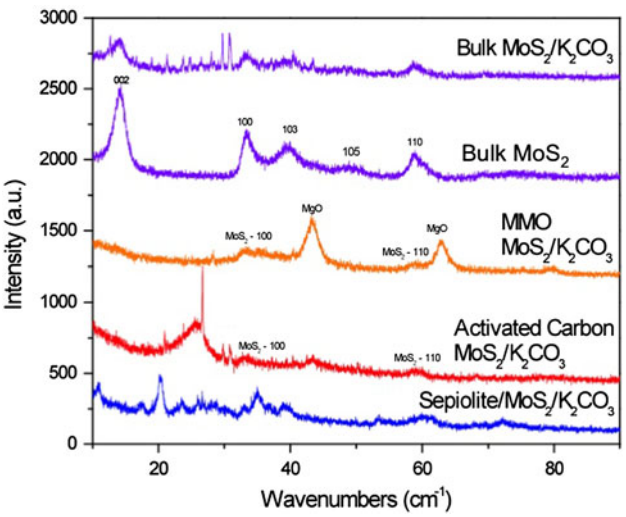

Fig. 1 XRD of supported and unsupported K_2CO_3 promoted MoS_2. Supported samples were sulfided in situ and reacted with syngas for 2–4 days

[1] There are several views on the appropriate H_2S concentration for catalytic higher alcohol synthesis using MoS_2-based materials. Stevens et al. [34] stated that H_2S levels below 100 ppm would not significantly affect the structure of MoS_2 materials and that at levels above that concentration "no advantage is realized." However, Christensen et al. [47] indicate that H_2S concentrations above 100 ppm cause the catalyst to stabilize more quickly and improve productivity, while simultaneously leading to higher hydrocarbon selectivities. Given this study's goal to obtain high alcohol selectivities while minimizing hydrocarbons, 50 ppm H_2S in the syngas feed was used.

as such, the observed bands may be considered identical. The stretches were less apparent in the activated carbon sample, most likely because the carbon support absorbed most of the light.

The BET surface areas (reported in Table 1) computed from nitrogen physisorption data show that the activated carbon and sepiolite catalysts lost surface area over the course of sulfidation and reaction. This result may be a consequence of sintering or carbon deposition. The MMO supported catalyst showed a slight increase in BET surface area, but the difference is considered to be within the error of the measurement. The bulk, MMO, and sepiolite supported catalysts showed small changes in post-reaction molybdenum content (<±6 %), while the activated carbon supported catalyst showed a large change (51 %). Drops in Mo content support the hypothesis of carbon buildup on the catalyst surface. Due to its microporous nature, activated carbon is particularly susceptible to coke build-up in syngas reactions [49]. Nitrogen adsorption isotherms for the MMO supported catalyst at various stages are given in Fig. S1 in supporting information. Pore blockage from hydrocarbon wax build up is also a possible cause for reduced surface areas, but volatile product analysis reveals only low molecular weight hydrocarbon species and there were no waxes found in downstream traps.

The results of the catalytic reactions are reported in Table 2. The transient data for the MMO supported catalyst are given in Fig. S2 in supporting information. The bulk MoS_2 catalyst showed high selectivity for both methanol and ethanol. This result is consistent with what was found in other studies [37, 50–52]. Additionally, methane accounted for most of the hydrocarbons produced over this catalyst. The MMO supported catalyst showed the greatest $C_{2+}OH$ selectivity at 55.5 %, in addition to the highest propanol and butanol selectivities. Most notable was the low methanol selectivity, which was uncharacteristically lower than the ethanol, *n*-propanol, and *n*-butanol selectivities. By comparison, the methanol selectivity on the MMO supported catalyst was almost eight times lower than that observed for the bulk MoS_2 catalyst. The MMO supported catalyst was less active than the activated carbon supported and bulk catalysts. Given the hypothesis that basic alkali block active sites, it is possible the MMO support interacts with the MoS_2 domains in a similar fashion.

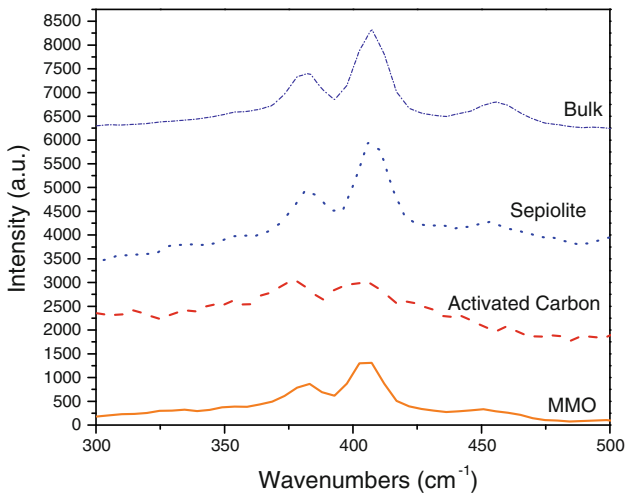

Fig. 2 Raman spectroscopy of the reaction-aged, sulfided catalysts using a 1,800 grating, 514 nm 1 mW laser

When activities are normalized per gram of molybdenum, the activated carbon supported catalyst was the most productive for higher alcohols, with an hourly productivity of 0.88 g-C_{2+}OH/g-Mo/h. The MMO and bulk samples had roughly the same activity, at 0.23 g-C_{2+}OH/g-Mo/h, and the sepiolite sample was the least active at 0.06 g-C_{2+}OH/g-Mo/h. Of the supports used in this study, activated carbon was the least basic as shown by CO_2 TPD (supporting information). While it is not fully established whether support basicity has a similar effect on catalytic activity and selectivity as alkali, it is noteworthy that the most neutral support, activated carbon, had the highest activity while the most basic support, MMO, had the lowest. While catalytic activity did appear to correlate with support basicity, other factors, such as differences in MoS_2 dispersion among the different catalysts may also influence the results. Counter to this hypothesis, XRD shows that the supported catalysts are all highly dispersed, although further, more detailed investigations of the MoS_2 domains are needed.

The sepiolite supported catalyst was highly selective for hydrocarbons, most likely due to its high acid site content as shown by NH_3 TPD (supporting information). A similar result was observed when syngas was reacted over acidic alumina and silica supported MoS_2 [31]. While CO_2 TPD shows the catalyst does possess some basic sites, we hypothesize that the acid sites are not adequately neutralized at the potassium levels used here, and hence hydrocarbon formation is more highly favored in the reaction of syngas over this catalyst under these conditions.

Interestingly, the methanol selectivity was lower for both the carbon and MMO supported catalyst than for the bulk catalyst. However, the MMO supported catalyst yielded selectivities that were much more strongly biased towards C_{3+} alcohols than any of the other catalysts.

The Anderson–Shultz–Flory distribution of the alcohols in Fig. 3 shows that the MMO supported catalyst deviates substantially from the trend shown for ethanol, *n*-propanol, and *n*-butanol. Additionally, the chain growth parameter, α, is the largest for the MMO supported sample among the catalysts studied, indicating a higher probability for longer chains than the unsupported catalyst and the two other

Table 1 Pre-reaction/sulfidation catalyst and sulfided, reaction aged catalyst compositions and surface areas measured via ICP and nitrogen physisorption respectively

Catalyst support	Oxide pre-reaction			Post-reaction sulfide catalyst		
	Mo (wt%)	K (wt %)	Surface area (m^2/g)	Mo (wt%)	K (wt%)	Surface area (m^2/g)
Bulk	30.3	14.5	89	29.8	14.5	–
MMO	5.2	2.1	71	4.9	2.1	78
Carbon	4.3	1.8	245	2.2	0.9	175
Sepiolite	4.4	2.9	102	4.5	2.5	70

Table 2 Reaction results of supported and unsupported MoS_2 catalysts

Support	GHSV (mL/g/h)	% Conv.	% Selectivity							$C_{2+}OH$ Prod ($g/g_{Mo}/h$)	Time on Stream (days)
			Organic products by carbon excluding CO_2								
			MeOH	EtOH	*n*-PrOH	*n*-BuOH	CH_4	$C_{2+}OH$	Tot. HC		
Bulk	8,004	8	34.1	32.9	5.5	0.9	19.6	39.3	22.2	0.23	3.4
MMO	1,377	8	4.5	25.9	18.7	10.9	13.9	55.5	37.0	0.23	3.0
Carbon	3,973	8	14.2	33.5	13.6	4.6	15.7	51.7	32.0	0.88	3.2
Sep	1,937	8	2.7	5.0	2.3	1.0	20.3	8.3	88.5	0.06	2.6

Reactions run at 1,500 psig, 310 °C, H_2:CO 1:1, 50 ppm H_2S. Gas hourly space velocity (GHSV) and productivity are reported in mL syngas/g-cat/h and g $C_{2+}OH$ per gram of Mo per hour, respectively

[a] Estimated error ±0.4 %

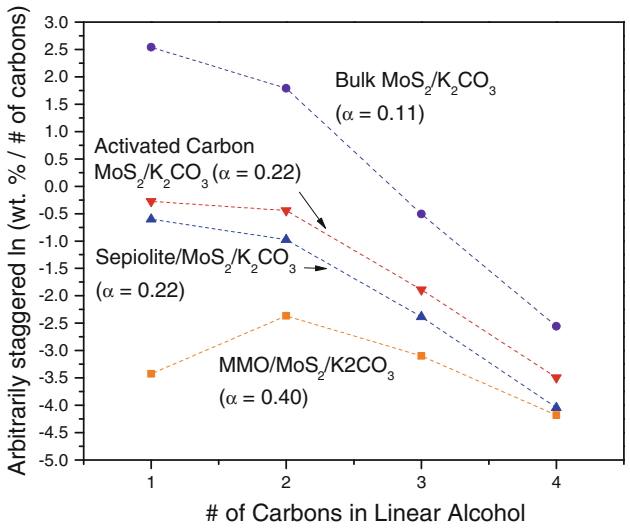

Fig. 3 The ASF distribution of alcohols on various supported and unsupported potassium promoted MoS_2 catalysts. The α values were computed for C_2–C_4 linear alcohols

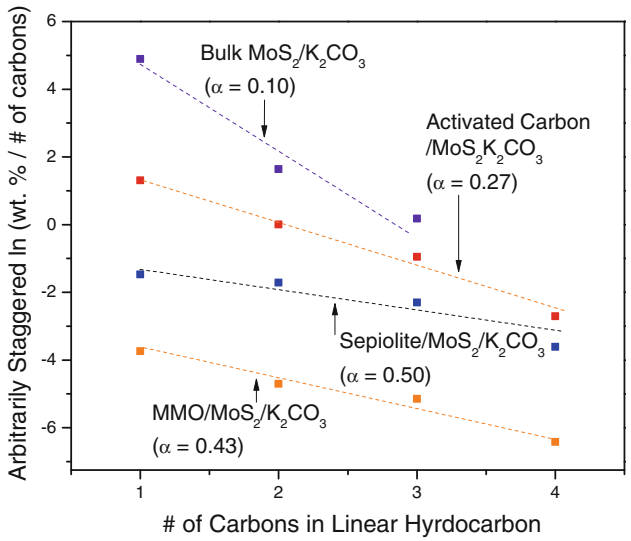

Fig. 4 The ASF distribution of hydrocarbons on various supported and unsupported potassium promoted MoS_2 catalysts. The α values were computed for C_1–C_4 linear hydrocarbons on supported catalysts and C_1–C_3 for bulk MoS_2

supported catalysts. The ASF distriution shown in Fig. 4 for hydrocarbons reveals that the MMO supported catalyst possessed a greater chain growth probability than the activated carbon and bulk catalysts. There are a multitude of possible explanations for these observations. These include hydrogenation of methanol to form methane. However, as shown in Fig. 4, methane selectivity seems to follow the ASF trend. Alternatively, some form of metal–oxide promoted alcohol coupling could contribute to the ASF distribution of alcohols on the MMO catalyst. This phenomenon has been observed on transition metal free $Mg_xAl_xO_x$ [53] and on a Cu/ZnO catalyst [14, 15]. In addition, Christensen et al. [54] showed that alcohol coupling was possible over CoMoS when an ethanol co-feed

was used in conjunction with syngas. In that work, reactions showed increased *n*-butanol and *n*-propanol selectivity in addition to higher selectivities for higher hydrocarbons. Although these findings are not directly analogous to syngas reactions over MMO supported MoS_2, they suggest that there are multiple potential pathways that may contribute to the unique product distributions observed in this work beyond traditional CO insertion [55].

Another possibly complementary explanation of the uncharacteristically low methanol selectivity observed on the potassium-promoted, MMO supported MoS_2 catalyst may be associated with the capacity of metal oxides, MgO in particular, to decompose methanol to H_2, CO, and CO_2 [56, 57]. Goodarznia et al. [58] showed that C_2 oxygenates such as methyl formate and ethanol could be formed from methanol alone when MgO was combined with potassium and copper. MMO supported MoS_2 may possess a similar capacity.

Finally, low methanol selectivity may possibly be explained as an artifact of basicity—whether it comes from the support or from an alkali promoter. Several studies that investigated the impact of potassium loading found that the methanol to ethanol ratio reached a minimum around the level that potassium loading was optimal for higher alcohol productivity [6, 30, 59, 60]. Ultimately, additional investigation is needed to better understand the nature of higher alcohol formation on the MMO supported MoS_2 catalyst.

4 Conclusions

It has been demonstrated that MMO supported K/MoS_2 materials bring unique aspects to catalytic mixed alcohol synthesis from syngas. First, the catalyst allows for lower methanol selectivity, well below the values predicted by the ASF distribution. Second, the catalyst increases alcohol chain growth, yielding high selectivities for *n*-propanol and *n*-butanol. The relative and possibly complementary effects of the alkali promoter and MMO support as well as the mechanism(s) leading to the unique product selectivity are not, at this early stage, fully understood, but this material appears to be a promising composition for further study.

Acknowledgements The authors express gratitude to The Dow Chemical Company for financial support of this work.

References

1. Mills AG (1994) Fuel 73:1243
2. Fischer F, Tropsch H (1926) Chem Ber 59:830
3. Surisetty VR, Dalai AK, Kozinski J (2011) Appl Catal A 404:1
4. Garbow IC, Mavrikakis M (2011) ACS Catal 1:365
5. Gupta M, Smith ML, Spivey JJ (2011) ACS Catal 1:641
6. Woo HC, Park KY, Kim YG, Nam I-S, Chung JS, Lee JS (1991) Appl. Catal. 75:267
7. Lui Z, Li X, Close MR, Cugler EL, Pertersen JL, Dadyburjor DB (1997) Ind Eng Chem Res 36:3085
8. Youchang X, Naasz BM, Somorjai GA (1986) App. Catal. 27:233
9. Murchison CB, Conway MM, Stevens RR, Quarderer GJ (1988) In: 9th international congress on catalysis, Calgary
10. Yang Y, Wang Y, Liu S, Song Q, Xie Z, Gao Z (2009) Catal Lett 127:448–455
11. Bao J, Fu Y-L, Bian G-Z (2008) Catal Lett 121:151
12. Ma X, Lin G, Zhange H (2006) Catal Lett 111:141
13. Zhang Y, Sun Y, Zhong B (2001) Catal Lett 76:249
14. Nunan JG, Bogdan CE, Klier K, Smith KJ, Young CW, Herman RG (1988) J Catal 113:410
15. Nunan JG, Bogdan CE, Klier K, Smith KJ, Young C, Herman RG (1989) J Catal 116:195
16. Nunan JG, Herman RG, Klier K (1989) J Catal 116:222
17. Haider MA, Gogate MR, Davis RJ (2009) J Catal 261:9
18. Schwartz V, Campos A, Egbebi A, Spivey JJ, Overbury SH (2011) ACS Catal 1:1298
19. Arakawa H, Fukushima T, Ichikawa M, Natsushita S, Takeuchi K, Matsuzaki T, Sugi Y (1985) Chem Lett 7:881
20. Bian G, Fu Y, Ma Y (1999) Catal Today 51:187
21. Muramatsu A, Takashi T, Tominaga H (1987) Bull Chem Soc Jpn 60:3157
22. Fang K, Li D, Lin M, Xiang M, Wei W, Sun Y (2009) Catal Today 147:133
23. Spivey JJ, Egbedi A (2007) Chem Soc Rev 36:1514
24. Subramani V, Gangwal SG (2008) Energy Fuel 22:814
25. Gang L, Chengfang Z, Yanqing C, Zhibin Z, Yianhui N, Linjun C, Fong Y (1997) Appl Catal A 150:243
26. Wu X-M, Guo Y–Y, Zhou J-M, Lin G-D, Dong X, Zhang H-B (2008) Appl Catal A 340:87
27. Iranmahboob J, Hill DO (2002) Catal Lett 78:49
28. Iranmahboob J, Hill DO, Toghiani H (2001) Appl Surf Sci 185:72
29. Surisetty VR, Tavasoli A, Dalai AK (2009) Appl Catal A 365:243
30. Zhang JY, Wang YJ, Chang L (1995) Appl Catal A 126:1205
31. Bian G-Z, Fan L, Fu Y-L, Fujimoto K (1998) Ind Eng Chem Res 37:1736
32. Lowenthal E, Schwarz S, Foley HC (1995) J Catal 154:96
33. Lee JS, Kim S, Lee KH, Nam IS, Chung JS, Kim YG, Woo HC (1994) Appl Catal A 110:11
34. Stevens RR (1988) Process for producing alcohols from synthesis gas. U.S. Patent 4752622
35. Woo HC, Nam I-S, Lee JS, Chung JS, Lee KH, Kim YG (1992) J Catal 138:525
36. Dianis WP (nd) Appl Catal 30:99
37. Li D, Yang C, Li W, Sun Y, Zhong B (2005) Top Catal 32:233
38. Bezen MCI, Breitkopf C, Lercher JA (2011) ACS Catal 1:1384
39. Valente J (2000) J Catal 189:370
40. Fishel CT, Davis RJ (1994) Catal Lett 25:87
41. Lei X, Zhang F, Yang L, Guo X, Yuanyuan T, Fu S, Li F, Evans DG, Duan X (2007) AICHE 54:932
42. Meloni D, Monaci R, Solinas V, Auroux A, Dumitriu E (2008) Appl Catal A 350:86
43. Prinetto F, Ghiotti G, Graffin P, Tichit D (2000) Microporus Mesoporus Mater 39:229–247
44. Takehira K (2004) Catal Commun 5:209
45. Perez-Ramirez J, Abello S, van der Pers NM (2007) Chem-Eu J 13:870
46. Iranmahboob J, Toghiani H, Hill DO (2003) Appl Catal A 247:207
47. Christensen JM, Mortensen PM, Trane R, Jensen PA, Jensen AD (2009) Appl Catal A 366:29
48. Muller A, Weber T (1991) Appl Catal 77:243
49. Surisetty VR, Dalai AK, Kozinski J (2011) Energy Fuels 25:580

50. Nam I-S, Park TY, Kim YG (1997) Ind Eng Chem Res 36
51. Woo HC, Nam I-S (1993) J. S. L. A. J. S. Chung, Y. G. Kim. J Catal 142:672
52. Qi H (2003) Catal Commun 4:339–342
53. Cosimo JID, Apesteguia CR, Gines MJL, Iglesia E (2000) J Catal 190:261
54. Christensen JM, Jensen PA, Schiødt NC, Jensen AD (2010) ChemCatChem 2:523
55. Santiesteban JG, Bogdan CE, Herman RG, Klier K (1988) In: 9th annual congress on catalysis, Calgary, p 561
56. Bowker M, Houghton H, Waugh KC (1981) J Chem Soc Faraday Trans 1:77
57. Tsoncheva T, Ivanova L, Minchev C, Froba M, Col J (2009) Intf Sci 333:277
58. Goodarznia S, Smith KJ (2010) J Mol Catal A 320:1
59. Jiang M, Bian G-Z, Fu Y-L (1994) J Catal 146:144
60. Calverley EM, Smith KJ (1991) J Catal 130:616